**Beam Physics Note**
TRI-BN-24-18
July 29, 2024

# Measurement of beam energy from e-gun at TRIUMF e-linac

H. W. Koay

TRIUMF

**Abstract:** This work reports the measurement of beam energy using solenoids for low-energy electron beams.

# 1 Introduction

The nominal HV bias of the e-Linac thermionic gun is 300 keV. However, the readback is consistently showing some deviation. We need a reliable way to validate this value. In this case, the solenoid is a good tool to measure the energy due to its consistent $B_s$ d$s$ that is independent from any offset or hysteresis. Motivated by the successful application of this idea in [1], this study aims to perform a similar measurement to determine the beam energy from the e-gun.

# 2 Calculation of beam energy

The Larmor angle, $\theta_r$, between the particle's rotating frame and the stationary laboratory system can be written as:

$$\theta_r = \int \frac{qB_s \mathrm{d}s}{2p} = \int \frac{B_s \mathrm{d}s}{2B\rho} \tag{1}$$

For a solenoid of a finite length $L$ and radius $R$, $B_s$ can be expanded as follows for small offset $r$,[2, 3]:

$$B_s = B_s(0,s) - \frac{r^2}{4}\frac{\mathrm{d}^2 B_s(0,s)}{\mathrm{d}s^2} + ... \tag{2}$$

$$B_s(0,s) = \frac{\mu_0 N I}{2L}\left[\frac{z+\frac{L}{2}}{\sqrt{R^2+(z+\frac{L}{2})^2}} - \frac{z-\frac{L}{2}}{\sqrt{R^2+(z-\frac{L}{2})^2}}\right] \tag{3}$$

When solving the integral of 2 to infinity, it is consistent with the Ampere's Law of $\int_{-\infty}^{\infty} B_s \mathrm{d}s = \mu_0 N I$ [Appendix C]. **This holds even for** $r \neq 0$, as $r \ll z$, and $z \to \pm\infty$ in most cases.

For instance, taking the numerical integral of the on-axis component for ELBT:SOL1. The plot is also shown in Fig. 1. The integral $\int_{-200\,\mathrm{mm}}^{200\,\mathrm{mm}} B_s(0,s)\mathrm{d}s$ is about 2.6 Tmm. To verify it against Ampere's Law, the solenoid has 660 turns, each at 3.09 A, $B_0 = \mu_0 N I =$ 2.56 Tm. The two values are consistent with each other.

Now, let's assume that the beam passes through the solenoid at an offset $r = 10$ mm. Assume the off-axis term as given in eqn 2, $\frac{r^2}{4}\frac{\mathrm{d}^2 B_s(0,s)}{\mathrm{d}s^2}$, we can determine its contribution to $\int B_s \mathrm{d}s$ by numerically solving the integral of the second derivative. As shown in Fig. 1, $\int_{-200\,\mathrm{mm}}^{200\,\mathrm{mm}} \frac{r^2}{4}\frac{\mathrm{d}^2 B_s(0,s)}{\mathrm{d}s^2}\mathrm{d}s$ is on the order of 0.00001. This is negligible as compared to the first term, despite an offset of 10 mm is considered significant during usual beam delivery. Therefore, it is confirmed that the centroid will always be rotated by $\theta_r$ regardless of the beam offset.

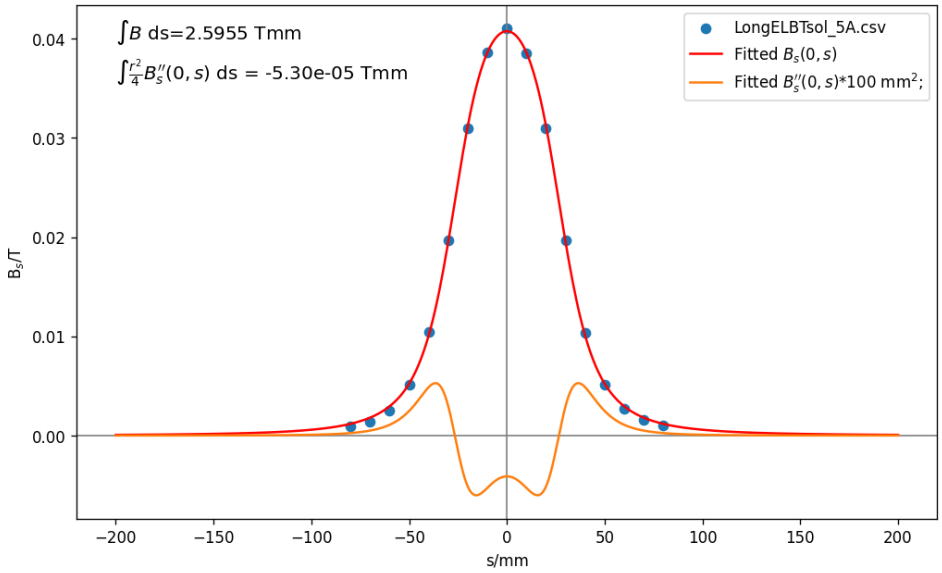


Figure 1: The on-axis magnetic field for ELBT:SOL1 at I=3.09 A.

# 3 Method

This work was initially performed on 02/07/2024. It was repeated again on 10/7/2024 due to discrepancy in X and Y measurements. Only the latest work is described here.

1. Set the EGUN:BIAS to 300 kV.
2. Set all the solenoids downstream of EGUN:SOL1 to 0 A. Investigate the best setting for EGUN:SOL1. For this study, EGUN:SOL1 is set to 2.65 A.
3. Set the pulse length to be 1 $\mu$s long.
4. Send the electron beam to ELBT:VS0. Ensure that the beam is well centered through solenoid.
5. Set EGUN:XCB0 to -0.4 A and take the snapshot of the VS image using the e-snapshot program in the automation code.
6. Repeat step 5 by changing EGUN:XCB0 with a step of +0.02 A.
7. Repeat step 5-6 by using EGUN:YCB0.
8. Repeat step 3-7 with EGUN:SOL1 set to +2.65 A.
9. Measurements are repeated for EGUN:BIAS at 270 kV. .
10. Similar works are repeated for EGUN:SOL1 and EGUN:VS1, ELBT:SOL1 and ELBT:VS2, as well as EGUN:SOL2 and ELBT:VS2.

# 4 Results and discussions

The beam centroid at different solenoid currents are plotted for the horizontal and vertical steer respectively $\Delta\theta$ is the angle between the two scans of opposite solenoid polarities. From eqn 1, we can determine the beam energy (from its rigidity) using

$$\begin{aligned}\Delta\theta &= \frac{\int B_s - (-B_s)\mathrm{d}s}{2B\rho} \\ &= \frac{\int B_s \mathrm{d}s}{B\rho} \\ B\rho &= \frac{\int B_s \mathrm{d}s}{\Delta\theta}\end{aligned} \tag{4}$$

The result is shown in Fig. 2. $\Delta\theta$ are 73.62° and 74.84° for the horizontal and vertical steerer, respectively. Taking these $\Delta\theta$, the beam energy lies between 0.301 and 0.293 MeV. This is consistent with the set-point and readback values we see in EPICS.

Similar analysis were also performed using ELBT:SOL1 and ELBT:SOL2, respectively. The results are shown in Fig. 3 and 4.

From Fig. 4, similar energy range is obtained. This further validates our previous calculations using EGUN:SOL1. On the other hand, as for ELBT:SOL1 and ELBT:VS2, there is a significant discrepancy between the X and Y measurements as shown in Fig. 3. The reasons is not yet known so this set of data is set aside for future investigations.

Furthermore, another measurement was also done for a 270 keV beam using EGUN:SOL1. The result is given in Fig. 5. $\Delta\theta$ are 74.03° and 75.44° for the horizontal and vertical steerer, respectively. The range also agrees with the ±40 keV that we observed so far. The corresponding beam energy lies between 0.271 and 0.263 MeV.

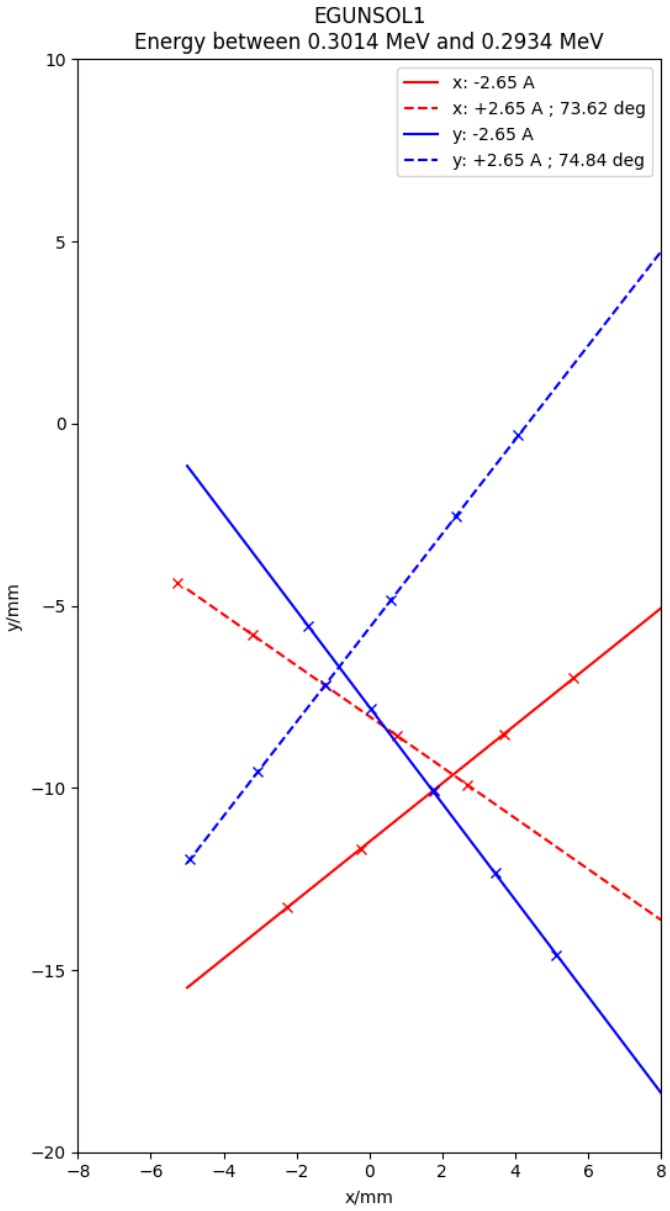


Figure 2: Beam centroids when EGUN:SOL1 was set to ±2.65 A. The EGUN:BIAS was set to 300 kV. The corresponding lines are fitted and the rotation angle $\Delta\theta$ between the positive and negative currents are evaluated. $\Delta\theta$ between the two scans with the opposite solenoid polarities are 73.62° and 74.84° for the horizontal and vertical steerer, respectively.

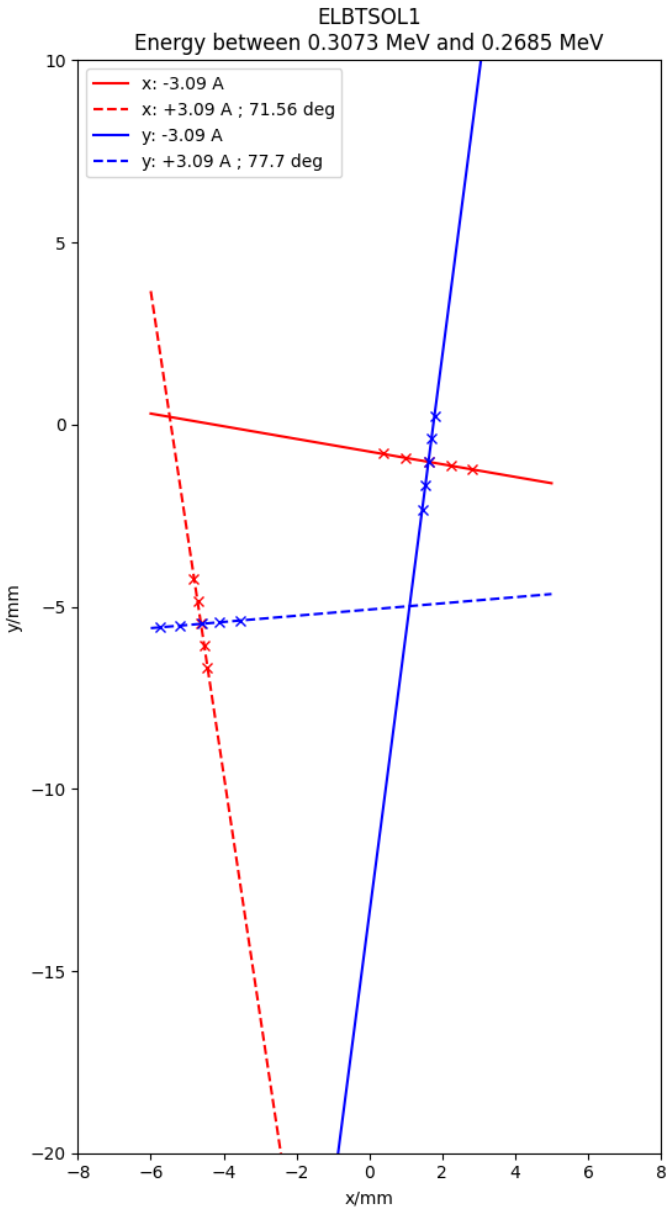


Figure 3: Measured beam centroids during the scans of the ELBT:XCB0 (horizontal;red) and ELBT:YCB0 (vertical;blue) steerers when ELBT:SOL1 was set to ±3.09 A respectively. The EGUN:BIAS was set to 300 kV. $\Delta\theta$ between the two scans with the opposite solenoid polarities are 71.56° and 71.7° for the horizontal and vertical steerer, respectively. The discrepancy remains unknown.

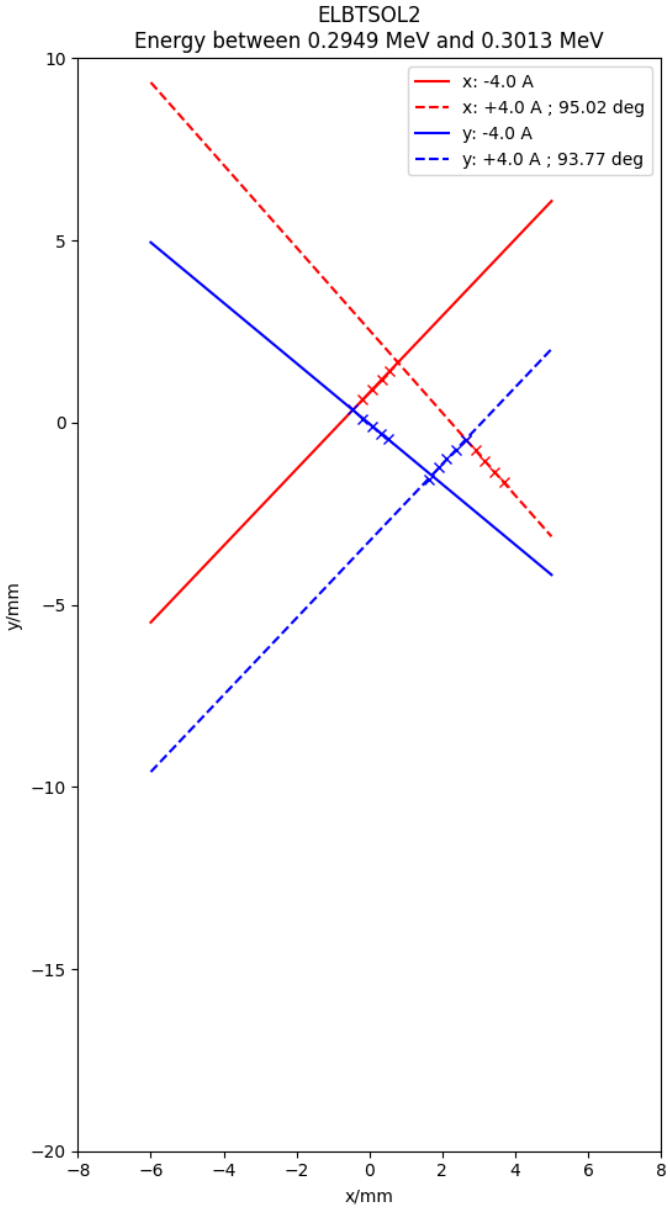


Figure 4: Beam centroids when ELBT:SOL2 was set to ±4.0 A. EGUN:BIAS was set to 300 kV. $\Delta\theta$ between the two scans with the opposite solenoid polarities are 95.02° and 93.77° for the horizontal and vertical steerer, respectively.

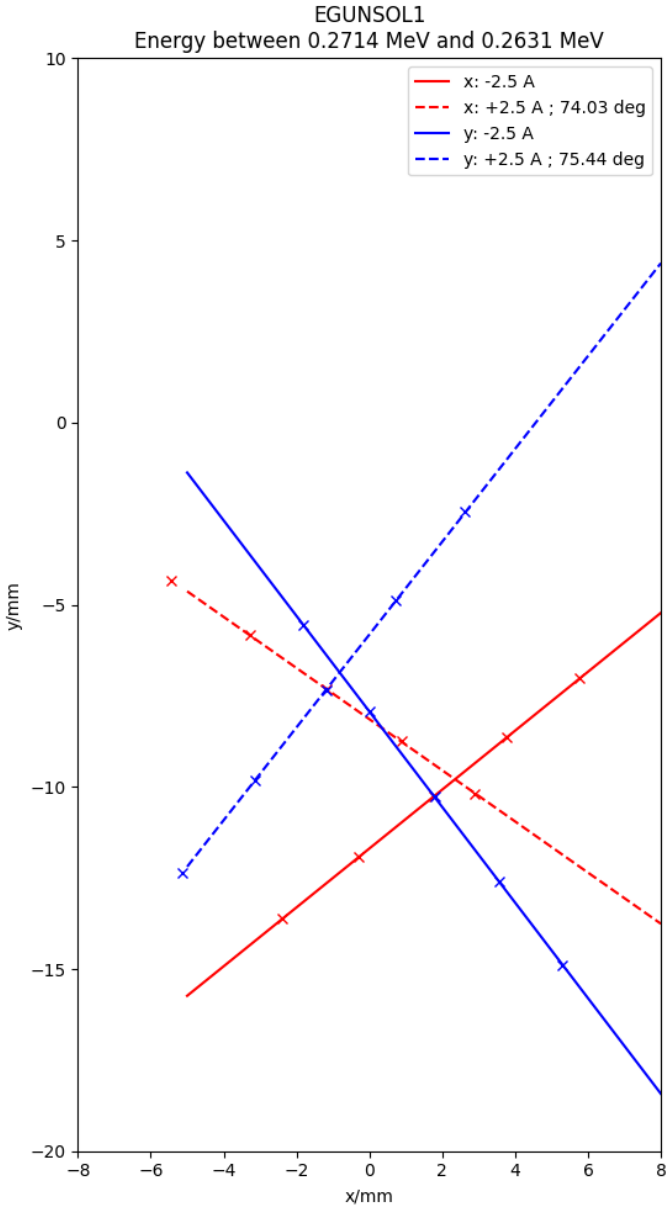


Figure 5: Beam centroids when EGUN:SOL1 was set to ±2.5 A. The EGUN:BIAS was set to 270 kV. $\Delta\theta$ between the two scans with the opposite solenoid polarities are 74.03° and 75.44° for the horizontal and vertical steerer, respectively.

# 5 Conclusions

In conclusion, the beam energy measured using solenoids agree with EGUN:BIAS set-point and readback shown in EPICS. When EGUN:BIAS is 300 keV, the beam energy is $29.8 \pm 0.3$ keV; while $26.7 \pm 0.4$ keV when EGUN:BIAS is set to 270 keV. More works are needed to understand the discrepancy in Fig. 3.

# References

[1] I. Pinayev, Y. Jing, D. Kayran, V. N. Litvinenko, J. Ma, K. Mihara, I. Petrushina, K. Shih, G. Wang, Y. H. Wu, Using solenoid as multipurpose tool for measuring beam parameters, Review of Scientific Instruments 92 (1) (2021) 013301. arXiv:https://pubs.aip.org/aip/rsi/article-pdf/doi/10.1063/5.0015618/13510043/013301_1_online.pdf, doi:10.1063/5.0015618.
URL https://doi.org/10.1063/5.0015618

[2] J. D. Jackson, Classical electrodynamics, John Wiley & Sons, 2021.

[3] P. Martín-Luna, B. Gimeno, D. González-Iglesias, D. Esperante, C. Blanch, N. Fuster-Martínez, P. Martinez-Reviriego, J. Fuster, On the magnetic field of a finite solenoid, IEEE Transactions on Magnetics 59 (4) (2023) 1–6. doi:10.1109/TMAG.2023.3250837.

# A Benchmark against Automation and collection VS images

The measurement of beam centroid from VS was performed using the automated apps developed by previous co-op students. The code can be found in TRIUMF gitlab.

I performed a quick check to compare my calculated gradient with the one obtained from the code. A sample result is shown in Fig. 6. The two sets of processed centroid overlapped almost entirely on each other. The calculated gradient agree with each other up to 0.1%. This shows that the image processing is comparable to human process. Therefore, I used this program to generate all the beam centroid from view screens.

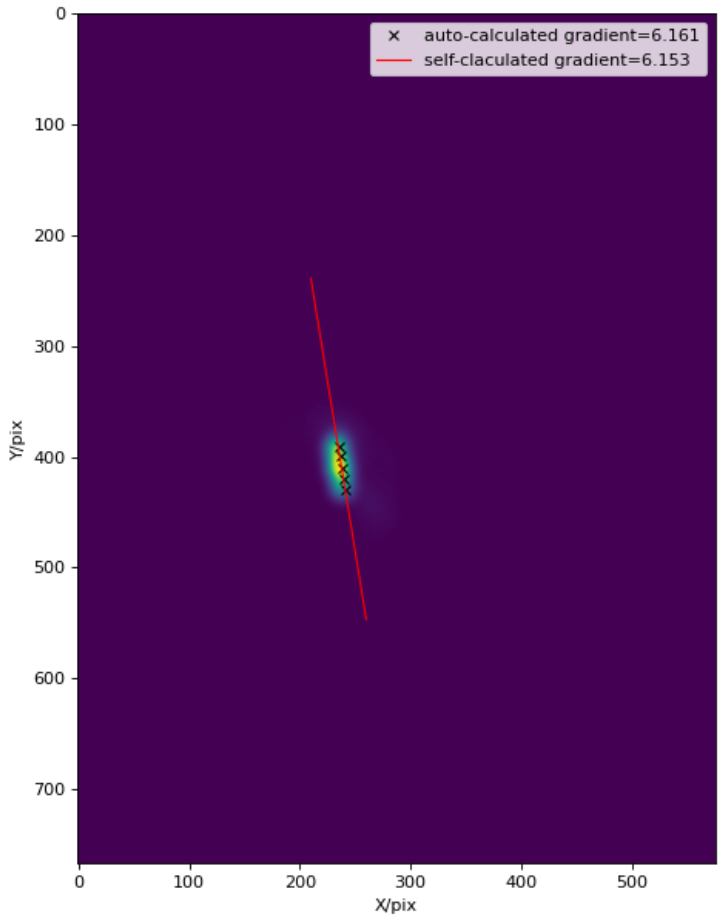


Figure 6: Stacking images of five different values of ELBT:XCB0:CUR from -0.04 A to 0.04 A. All images were taken at ELBT:VS2. Red lines showed the self-calculated centroid, while black crosses are the auto-calculated centroids. Both the absolute coordinate and the gradients agree well in both calculations.

# B Steering the beam when solenoid is set to 0 A

The slight discrepancy between X and Y steer through ELBT:SOL1 indicates a potential external quadrupole effect. To check this, the beam was steered by ELBT:X/YCB0 with both ELBT:SOL1 and ELBT:SOL2 set to 0 A. Then, the centroid of the direct steered beam on ELBT:VS2 were recorded. The results are shown in Fig. 7

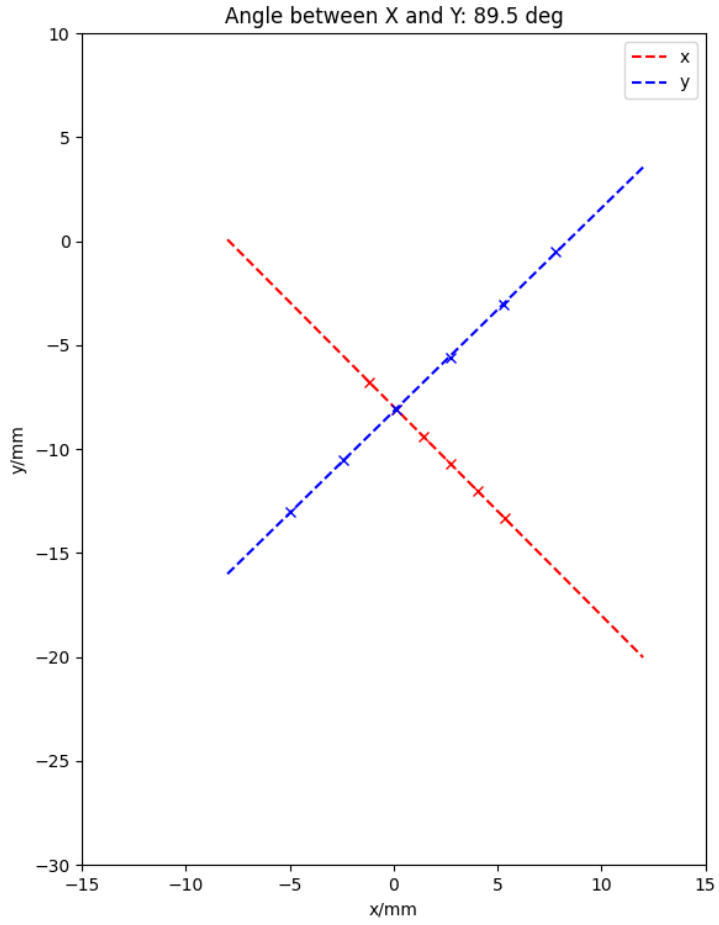


Figure 7: The plot of beam steered by ELBT:XCB0 and YCB0 respectively. All the downstream solenoids were set to zero.

From Fig. 7, the steered beam is highly linear. This shows that the quarupole effect is actually minimal. However, the X and Y steer do not steer the beam in the exact horizontal and vertical directions. Instead, it is at 45° and 135°.

# C Solving the integral of solenoid field up to the second order

Taking the integral of the axial magnetic field in eqn 2,

$$\int_{-\infty}^{\infty} B_s \mathrm{d}s = \int_{-\infty}^{\infty} B_s(0,s)\mathrm{d}s - \int_{-\infty}^{\infty} \frac{r^2}{4}\frac{\mathrm{d}^2 B_s(0,s)}{\mathrm{d}s^2}\mathrm{d}s \tag{5}$$

Solving the first term on RHS, we have

$$\int_{-\infty}^{\infty} B_s(0,s)\mathrm{d}s = \frac{\mu_0 NI}{2L}\left[\sqrt{R^2+(z+\frac{L}{2})^2} - \sqrt{R^2+(z-\frac{L}{2})^2}\right]_{-\infty}^{\infty}$$

As $B_s(0,s)$ is symmetry in z, it can also be written as

$$\int_{-\infty}^{\infty} B_s(0,s)\mathrm{d}s = \frac{\mu_0 NI}{L}\left[\sqrt{R^2+(z+\frac{L}{2})^2} - \sqrt{R^2+(z-\frac{L}{2})^2}\right]_{0}^{\infty}$$

At $z >> R$, $\sqrt{R^2+(z-\frac{L}{2})^2} \approx z-\frac{L}{2}$, and $\sqrt{R^2+(z+\frac{L}{2})^2} \approx z+\frac{L}{2}$,

$$\int_{-\infty}^{\infty} B_s(0,s)\mathrm{d}s \approx \frac{\mu_0 NI}{L}(L-0) = \mu_0 NI$$

Solving the second term of eqn 5,

$$\begin{aligned}
\int_{-\infty}^{\infty} \frac{r^2}{4}\frac{\mathrm{d}^2 B_s(0,s)}{\mathrm{d}s^2}\mathrm{d}s &= 2\left[\frac{r^2}{4}\frac{\mathrm{d}B_s(0,s)}{\mathrm{d}s}\right]_0^{\infty} \\
&= \frac{r^2}{2}\frac{\mu_0 NI}{2L}\left[\frac{(z+\frac{L}{2})^2}{\left(R^2+(z+\frac{L}{2})^2\right)^{3/2}} + \frac{1}{\sqrt{R^2+(z+\frac{L}{2})^2}}\right. \\
&\quad \left. -\frac{(z-\frac{L}{2})^2}{\left(R^2+(z-\frac{L}{2})^2\right)^{3/2}} + \frac{1}{\sqrt{R^2+(z-\frac{L}{2})^2}}\right]_0^{\infty} \\
&= 0
\end{aligned}$$